Proceedings of the 2003 IEEE/RSJ
Intl. Conference on Intelligent Robots and Systems
Las Vegas, Nevada · October 2003

Development of an Ultrasonic Clutch for Multi-Fingered Exoskeleton Haptic Device using Passive Force Feedback for Dexterous Teleoperation

Tatsuya Koyama[1], Kenjiro Takemura[2], Takashi Maeno[3]

[1] *Keio University, Yokohama, Japan, tkoyama@mmm-keio.net*
[2] *Tokyo Institute of Technology, Yokohama, Japan, kenjiro@mmm-keio.net*
[3] *Keio University, maeno@mech.keio.ac.jp*

Abstract

A novel multi-fingered exoskeleton haptic device using passive force feedback has been proposed by the authors. The haptic device solves the conventional problems of previously developed master-slave systems with force feedback, such as oscillations, complex structures and complicated control algorithm. However, some problems still remain in the conventional passive elements. In the present paper, an ultrasonic clutch for multi-fingered exoskeleton haptic device with passive force feedback function is developed. The ultrasonic clutch can solve problems of conventional passive elements, such as time delay, instability, and large size, by using unique characteristics of ultrasonic motor, as fast response, silent motion, and non-magnetic feature. It can also be designed to be smaller than conventional elements due to its simple structure. The clutch locks or releases the rotor by use of ultrasonic levitation phenomenon. First, we have designed the structure of the ultrasonic clutch using an equation of ultrasonic levitation phenomenon, results from structural analysis and finite element (FE) analysis of piezoelectric material of the vibrator. Then we have manufactured the ultrasonic clutch and have conducted a driving experiment. Finally, we have demonstrated that the maximum levitation force is around 20 N and the static friction torque of the ultrasonic clutch is up to 0.14 Nm.

1. Introduction

For the past decade, several haptic devices with force feedback function have been developed and now in practice [1]-[8]. The previously developed haptic devices are divided into two categories: i.e., an active force feedback system and a passive one. The active force feedback system mainly uses a bilateral control method. Actuators such as electromagnetic motor or hydraulic motor are used to perform bilateral force control, which enables us to manipulate an object dexterously using tele-robot. However, there is a potential problem that the system may harm the operator if the system becomes out of control. Therefore, the entire active force feedback system becomes complicated and expensive to keep it safe from troubles mentioned above.

On the other hand, the passive force feedback system uses passive elements such as brake or electromagnetic clutch to provide the force. As the operator moves against the resistance by the passive element, the operator can feel the reaction force. The passive force feedback system becomes simple and safe because the passive element never harms the operator even if the system becomes out of control by some trouble. Moreover, in our previous study we have confirmed that the use of passive force feedback system instead of using the active force feedback system can reduce the time delay in signal transmission [9].

In our other study, we have developed a multi-fingered exoskeleton haptic device using passive force feedback [10] as shown in Figure 1. Besides our previous device, there are several conventional passive force feedback systems such as a system using an electromagnetic powder clutch [11] and a system using an ER brake [12] as typical examples (Table 1). Although they have unique characteristics, they still have several problems in the

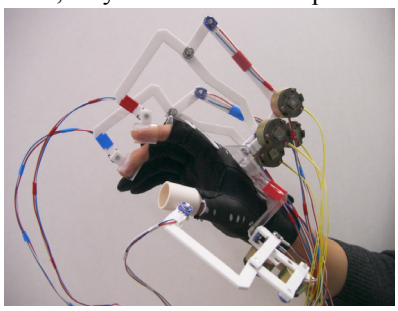

Figure 1: *Multi-fingered haptic device*

Table 1: *Specifications of conventional passive elements*

	ER brake	Electromagnetic clutch
Static friction torque [Nm]	6.3	0.25
Mass [kg]	2.6	0.065
Size [mm]	ϕ 156*135	ϕ 28*20
Response time [ms]	Several milliseconds	Several milliseconds

passive elements as follows:

Using electromagnetic powder clutch, torque can be easily controlled since the current which excites the coil is in proportion to the torque. However, since it takes several tens of milliseconds to respond, it is not suitable for high-speed control.

ER brake controls torque by use of rheology characteristic of its ER fluid. Namely, the viscosity of ER fluid changes inversely in proportion to the input voltage at high speed. However, ER brake is unable to provide torque when the operator stands still because it uses the viscosity of ER fluid to control torque.

We have used an electromagnetic clutch (Table 1) as a passive element on our previous haptic device. The weight of the electromagnetic clutch was so large that we could not place enough number of clutches on the haptic device to keep the operator free from fatigue. Furthermore, the electromagnetic clutch frequently becomes unstable due to electrical noise. Hence, the problems of conventional passive elements are summarized as follows:

(1) They are not highly responsive.
(2) Their motions are unstable.
(3) Their entire systems are large in size.

Therefore, it is necessary to develop a new type of passive element which solves the above-mentioned problems.

In the present study, a novel ultrasonic clutch is developed. The ultrasonic clutch solves the problems (1) and (2) by use of unique characteristics of ultrasonic motor such as fast response, silent motion and absence of electromagnetic feature. Moreover, the problem (3) is also solved since the ultrasonic clutch can be built smaller in size than the conventional ones due to simple structure of the vibrator. The ultrasonic clutch has the same unique features as ultrasonic motors; it uses an ultrasonic levitation phenomenon [13] for its operation. The ultrasonic levitation phenomenon is used for switching the state between lock/release of rotor and vibrator.

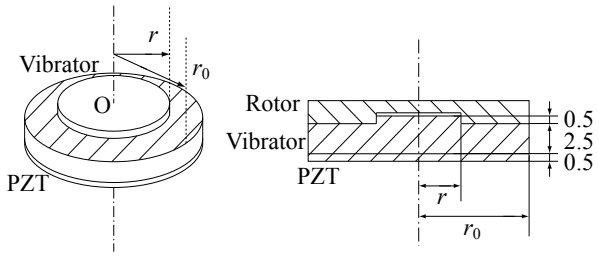

(a) Schematic view (b) Cross sectional view

Figure 2: *View of ultrasonic clutch*

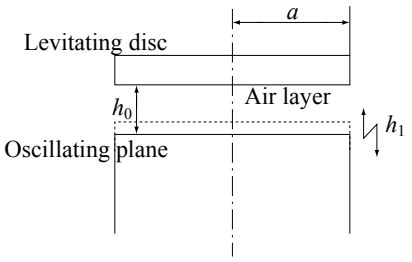

Figure 3: *Schematic view of levitating disc*

In this paper, the ultrasonic levitation phenomenon is introduced in chapter 2. The design of the ultrasonic clutch and the results of each analysis are mentioned in chapter 3. Then, the implementation of the ultrasonic clutch and the result of the driving test are described in chapter 4. The discussions and the future works are presented in chapter 5. Finally in chapter 6, the conclusions of this study are presented.

2. Ultrasonic Levitation Phenomenon

A schematic view of the vibrator is shown in Figure 2(a) and the cross sectional view of the clutch is shown in Figure 2(b). The figure does not show any other parts around the rotor and vibrator, however, a normal load is applied between rotor/vibrator by a spring to generate a static friction torque. The clutch uses the ultrasonic levitation phenomenon to levitate the rotor against the normal load to release the clutch. The clutch uses out-of-plane vibration to conduct the ultrasonic levitation phenomenon. Langevin's radiation pressure theory in acoustic field and squeeze film theory in lubrication field are the theories that explain the generation of the levitation force by the ultrasonic levitation phenomenon. Both theories are based on the use of vibration in ultrasonic range to levitate an object on an air layer. Therefore, the levitation force of the clutch can be calculated using above-mentioned theories.

A circular object with radius a is levitating with a small gap with a vibrating plane which has uniform displacement in whole plane (Figure 3), where the levitation force is obtained as follows [14]. By radiation pressure theory, it is calculated as

$$f_L = \int_0^a p_L \cdot 2\pi r dr = \frac{\pi a^2 \rho_0 c_0^{\,2}}{4}\left(\frac{h_1}{h_0}\right)^2 \qquad (1)$$

$$(h_1 / h_0 = 1)$$

On the other hand, the levitation force is obtained by squeeze film theory as

$$f_S = \int_0^a p_S \cdot 2\pi r dr = \frac{\pi a^2 \rho_0 c_0^{\,2}}{2\gamma} \qquad (2)$$

where

c_0 = Speed of sound in reference condition [m/s]

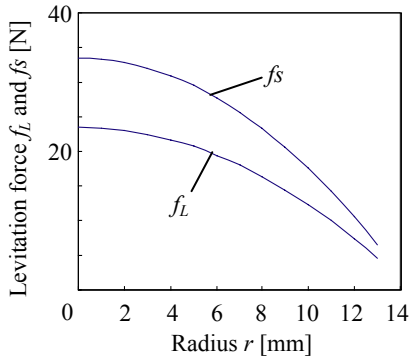

Figure 4: *Radius r vs. levitation force f_L and fs*

f_L = Levitation force by radiation pressure [N]
f_S = Levitation force by squeeze film [N]
h_0 = Levitation distance [m]
h_1 = Amplitude of vibrating plane [m]
p_L = Radiation pressure [Pa]
p_S = Time-average pressure of squeeze film [Pa]
γ = Ratio of specific heats
ρ_0 = Density of air in reference condition [kg/m^3]

Both equations (1) and (2) show the levitation forces are in proportion to the contact area of rotor and vibrator. Figure 4 shows the variation of levitation forces f_L and f_S against radius of the rotor r shown in Figure 2(a), where, maximum radius r_0 is 14 mm which we have decided based on the size of the electromagnetic clutch (Table 1) used in our previous haptic device. The variation range of the inner radius r is from 0 to 13 mm.

In addition, there has been a report that the squeeze film effect is more effective than the radiation pressure effect for the generation of the levitation force when the levitation distance is small [14]. The levitation distance of the clutch becomes small as the normal load increases up to several tens of Newton (as will be shown in chapter 3). Therefore, the levitation force is assumed to be generated by squeeze film effect. We design the clutch considering the levitation force calculated by squeeze film theory.

3. Design and Implementation

3.1 Design Condition

A design condition of the ultrasonic clutch must satisfy two points as follows in order to implement it in the haptic device. First, the static friction torque of the clutch should be around 0.20 Nm. Second, both mass and size of the clutch should be less than that of the electromagnetic clutch in Table 1. These two points have been already verified by our previous study [10].

The static friction torque T can be calculated as follows according to Coulomb's law

$$T = Fr \quad (F = \mu N) \tag{3}$$

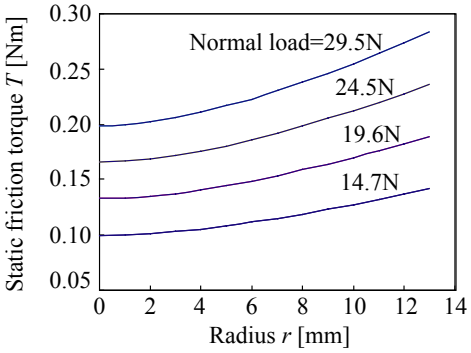

Figure 5: *Radius r vs. static friction torque T*

where F, r, μ and N are static friction force, radius, static friction coefficient and normal force, respectively. The pressure between rotor and vibrator is equally distributed by using a spring to set the normal load, so the static friction torque can be obtained by integrating equation (3) as follows

$$T = 2\pi\mu P\int_r^{r_0} r^2 dr \tag{4}$$

where P is the pressure. Figure 5 shows the variation of the static friction torque against the radius. The normal loads of the curves shown in Figure 5 are 14.7 N, 19.6 N, 24.5 N and 29.5 N, respectively. The static friction torque of the clutch is approximately in inverse proportion to the contact area of rotor and vibrator because the normal load on the rotor is equally distributed. Figure 5 indicates that the static friction torque increases as radius increases. Namely, the static friction torque becomes larger as the contact area becomes smaller. On the other hand, the levitation force is in proportion to the contact area, that means, small contact area cannot generate enough levitation force. Therefore, we decided the value of radius r as 4 mm, and also designed the shape of the contact area as striped area shown in Figure 2(a). This shape enables the vibrator to levitate normal load of 29.5 N because it can generate levitation force of around 30.9 N by squeeze film effect. It indicates that the static friction torque becomes 0.20 Nm and this satisfies the design conditions mentioned above. In addition, we designed the upper surface of the vibrator convexity to keep the center of the rotor and the vibrator correspond.

3.2 Finite Element Analysis

This section describes the result from structural analysis and FE analysis of piezoelectric material using finite element method in order to determine the characteristic of the designed vibrator.

First, the structural analysis was conducted. We made a finite element model of the vibrator. The brass, epoxy adhesive and lead zirconate titanate

Table 2: *Material properties*

	Brass	PZT	Epoxy adhesive
Young's modulus [GPa]	104.0	72.6	2.5
Poisson's ratio	0.33	0.31	0.40
Mass density [10^3kg/m^3]	8.6	7.7	2.3

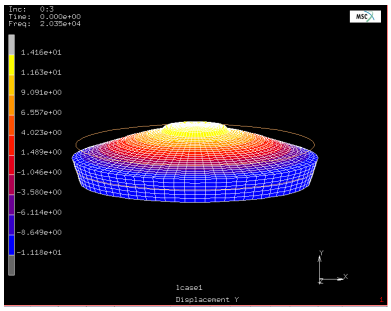

Figure 6: *Mode shape of vibrator*

(PZT) were adopted in the FE model. The material properties of each material are shown in Table 2. As a result of the structural analysis using above-mentioned model, the natural frequency of the out-of-plane vibration was 21.67 kHz and the mode shape is shown in Figure 6.

Next, a FE analysis of piezoelectric material was conducted. The input voltage and the frequency to the PZT of the analysis were 5.0 $V_{p\text{-}p}$ and 21.65 kHz, respectively. Moreover, we defined the damping ratio ζ as

$$\zeta = 1/2Q \tag{5}$$

where Q denotes the quality factor of the vibrator. The value of Q is around 1000 in general vibrator such as adhered brass and PZT so we used 1000 as Q. Figure 7 shows the distribution of the one side amplitude of vibration of the vibrator. As a result of the FE analysis of piezoelectric material, the amplitude of a point on the circumference of the upper surface was around 8.7 μm. According to an experiment in previous study [14], a 25 mm-by-25 mm plate weighing 700 g have successfully levitated using vibrating plane with amplitude of 5 μm and frequency of 20kHz. Therefore, the ultrasonic levitation phenomenon appears in case the amplitude is around 8.7 μm.

3.3 Implementation

The manufactured rotor and vibrator are shown in Figure 8. The rotor is also made of brass. The surface of both rotor and vibrator are coated by Nickel to protect the contact surface from wearing. Mass of the vibrator is 16 g. A device for driving

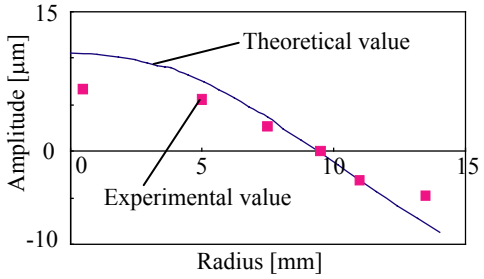

Figure 7: *Radius vs. amplitude*

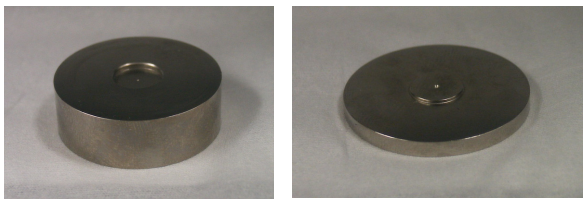

(a) Rotor (b) Vibrator

Figure 8: *View of manufactured rotor and vibrator*

experiment as shown in Figure 9 was also implemented. The device applies the normal load between the rotor/vibrator using coil springs. It is also designed to be capable of changing the magnitude of the normal load using a screw placed below.

4. Driving Test

This chapter describes the result from the driving test. First, we conducted a driving test without normal load to measure the amplitude of the upper surface of the vibrator. Next, we confirmed the relationship between the amplitude and the levitation force by conducting a driving test with various normal loads.

4.1 Driving Test without Normal Load

We measured amplitudes of six points on the upper surface (Table 3) of the vibrator using laser doppler vibrometer (GRAPHTEC, AT7211). The input voltage and the driving frequency to the vibrator were the same as the FE analysis of piezoelectric material (5.0 $V_{p\text{-}p}$, 21.65kHz). The result of this measurement is shown in Figure 7 to compare with the result of the FE analysis of piezoelectric material. Although there were some errors near the center and at the edge of the surface, we can confirm that the position of the node and the mode shape are well in agreement.

4.2 Driving Test with Normal Load

We confirmed the relationship between the amplitude and the levitation force by conducting a driving test with various normal loads using the device shown in Figure 9. The conditions of the

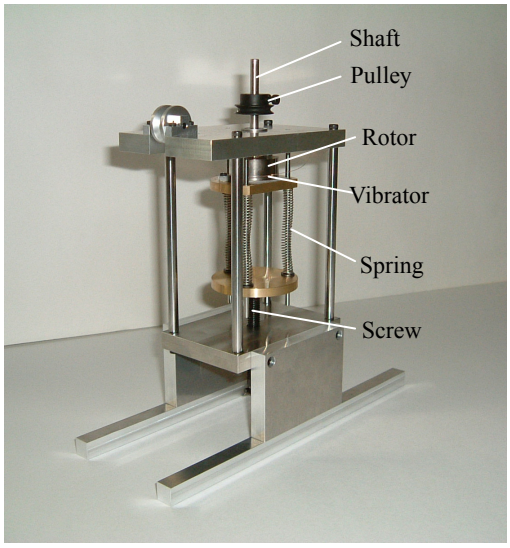

Figure 9: *View of device for driving test*

normal loads and the input voltage are as follows.

First, keeping the normal load at 5 various magnitudes as shown in Figure 12, we varied the input voltage from 20 V_{p-p} to 35 V_{p-p} in increments of 5 V_{p-p}. Next, we varied the normal load as 9.8 N, 14.7 N and 19.6 N, and then measured the input voltage and the amplitude which reduced the friction torque minimally. At the same time, we chose an appropriate driving frequency which matches with the resonant frequency because the resonant frequency generally changes with the variation of the magnitude of the input voltage. The amplitude of the measurement point 6 (Table 3) was measured as typical amplitude. The levitation forces in each experiment condition were obtained by hanging some weights to the pulley. In case the clutch is locked, the magnitude of the weight which is possible to be hanged to the pulley is in proportion to the normal load, and the magnitude of the weight is up to 2.3 kg maximally when the normal load is 29.5 N. Meanwhile, in case the clutch is released, the magnitude of the friction torque was confirmed that it reduced to less than $1.8*10^{-3}$ Nm due to the shaft had rotated when the weights of 2 g was hanged to the pulley. The friction torque of $1.8*10^{-3}$ Nm can be assumed as unloaded rotation compared to locked friction torque. Therefore, we defined the magnitude of the levitation force is the same as the magnitude of normal load when the friction torque became less than $1.8*10^{-3}$ Nm. The results of these measurements are shown in Figure 11 and Figure 12.

Figure 11 shows the relationship between the change of amplitude and the levitation force. Namely, it indicates that the normal load under the curve can be levitated in case the amplitude is constant. Moreover, the magnitude of the maximum levitation force was obtained as 19.6 N when the input voltage

Table 3: *Locations of measurement points*

Measurement point	1	2	3	4	5	6
Distance from center[mm]	0.5	5.0	7.5	9.5	11.0	13.5

was $45V_{p-p}$ and the driving frequency was 20.81kHz by changing the normal load. In addition, as the static friction coefficient between the rotor and the vibrator had been measured as 0.7 by the preliminary experiment, the maximum static friction torque is calculated as 0.14 Nm. Furthermore, in case we increased the magnitude of the normal load up to 29.5 N, we also confirmed that the clutch could reduce the friction torque under $1.8*10^{-3}$ Nm with the input voltage of 98 V_{p-p}. At the same time, the amplitudes were over 17 μm. However, we also confirmed that the PZT would crack if the amplitude increases over around 12 μm by the preliminary experiment. So the above-mentioned results with normal loads of 24.5 N and 29.5 N are supposed to be occurred with broken PZT. Therefore, we need to redesign the shape of the vibrator to levitate the normal load over 19.6 N safely.

Figure 12 shows the amplitude varied with input voltage under constant normal load. According to the result, the amplitude of vibration is in proportion to the input voltage. Therefore, a control of friction torque is able to be conducted by changing the input voltage under constant normal load.

As a result of the simulative calculation, the clutch generated a levitation force of around 30.9 N. However, the acquired levitation force was 19.6 N. The uneven shape of the vibrating plane of the vibrator is thought to be a main cause of the difference. Moreover, the ultrasonic levitation appears to incorporate several error factors such as surface roughness of the sliding surface and a shape of vibration.

5. Discussions and Future Works

In this paper, each driving test does not include transient measurements. Therefore, an accurate measurement of setting time of the ultrasonic levitation of the clutch is one of the future works. However, the settling time is inferred to be around several milliseconds from the characteristics of ultrasonic motors such as high speed. As a result from the driving test, we demonstrated that the steady-state levitation of the clutch is stable due to its non-magnetic feature. Meanwhile, stable static friction torque can also be generated due to normal load when the clutch is locked. Therefore, we can safely say that the clutch operates stably whether it is locked or released. A quantitative evaluation of the stability of the clutch and a comparison with the

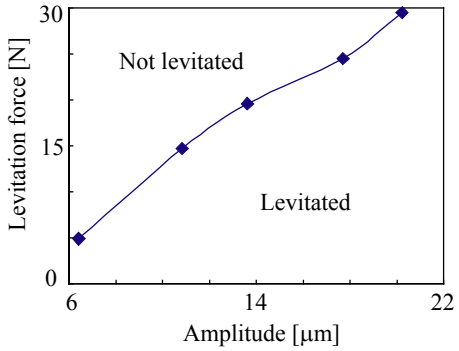

Figure 11: *Amplitude vs. levitation force*

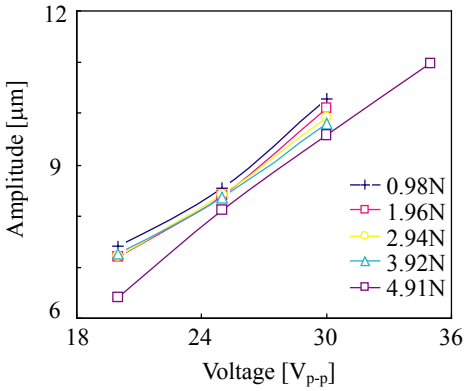

Figure 12: *Voltage vs. amplitude*

electromagnetic clutch should also be done in the future works. Although the mass of the vibrator is only 16 g, the clutch can generate static friction torque of 0.14 Nm. On the other hand, the mass of the electromagnetic clutch we used in the previous haptic device is 65 g and it generates static friction torque of 0.25 Nm. In case we implement the clutch in haptic device, the design of a unit composed of the rotor, vibrator and a shaft becomes a future work. However, we expect that the use of small conical spring washer and light weight material for the casing unit can make the entire size smaller and lighter. Therefore, we can say that the torque/inertia ratio of the developed ultrasonic clutch is much more superior to the conventional passive elements. Moreover, the ultrasonic clutch is capable of providing not only two states of lock/release but also a control of various magnitude of the friction torque, although the conventional electromagnetic clutches are unable to provide holding torque that varies continuously. Therefore, the novel clutch developed in this study can be used for high precision control device by properly controlling the driving characteristics. Furthermore, the redesign of the vibrator to generate a larger levitation force should also be done in the future works.

6. Conclusions

The ultrasonic clutch using out-of-plane vibration of vibrator for multi-fingered exoskeleton haptic device is developed in the present study. The levitation force is calculated using the equation from theories that explain the ultrasonic levitation. Furthermore, we have confirmed the natural frequency, mode shape and amplitude of the vibrator vibration by the structural analysis, frequency response analysis and FE analysis of piezoelectric material using FEM. From the driving test using the constructed ultrasonic clutch, it is demonstrated that maximum value of the levitation force is around 20 N and the static friction torque is up to 0.14 Nm.

References

[1] Grigore C. Burdea, *Force and touch feedback for Virtual Reality*, John Wiley & Sons, Inc., New York, 1996

[2] http://www.immersion.com/

[3] http://www.sensable.com/

[4] Gomez, D., G. Burdea, and N. Langrana, "Integration of the Rutgers Master II in a Virtual Reality Simulation", *IEEE Virtual Reality Annual Int. Symp. (VRAIS)*, pp.198-202, 1995

[5] S. C. Jacobsen, E.K. Iversen, D. F. Knutti, R.T. Johnson and K. B. Biggers, "Design of the Utah/MIT Dexterous Hand", *Proc. IEEE Int. Con. Robotics and Automation*, IEEE, pp.1520-1532, 1986

[6] http://www.cs.utah.edu/classes/cs6360-jmh/Nahvi/haptic.html#rm1

[7] http://www.sarcos.com/

[8] T. Kitada, Y. Kunii and H. Hashimoto, "20 DOF Five Fingered Glove Type Haptic Interface -Sensor Glove II-", *J. Robotics and Mechatronics*, Vol.9, No.3, pp. 171-176, 1997

[9] I. Yamano, K. Takemura, K. Endo and T. Maeno, "Method for Controlling Master-Slave Robots using Switching and Elastic Elements", *Proc. IEEE Int. Conf. on Robotics and Automation*, Vol. 2, pp. 1717-1722, 2002

[10] T. Koyama, I. Yamano, K. Takemura and T. Maeno, "Multi-Fingered Exoskeleton Haptic Device using Passive Force Feedback for Dexterous Teleoperation", *IEEE/RSJ International Conference on Intelligent Robots and System 2002*, Vol. 3, pp. 2905-2910, 2002

[11] O. Saito, K. Komoriya, R. Murata, "Passive Force Display with Powder Clutch", *Proc. of the 1998 JSME Conference on Robotics and Mechatronics*, No. 98-4, pp. 2AII1-6, 1998(in Japanese)

[12] K. Fukusumi, M. Sakaguchi, J. Furusho, "Basic Study on Passive Force Display", Proceedings of the 43nd Annual Conference of the Institute of Systems, Control and Information Engineers, ISCIE, pp. 305-306, 1999

[13] J. J. Blech, "On Isothermal Squeeze Films", ASME Jnl. of Lubrication Technology, Vol. 105, pp. 615-620, 1983

[14] K. Hashiba, K. Terao, T. Kunoh, "A Study on Ultrasonic Levitation", *XIXth International Congress of Theoretical and Applied Mechanics*, No. 1996-8, pp. 345, 1996